Coordination Chemistry Reviews 254 (2010) 2483–2491

Contents lists available at ScienceDirect

Coordination Chemistry Reviews

journal homepage: www.elsevier.com/locate/ccr

Review

Electrocatalytic and photocatalytic water oxidation to dioxygen based on metal complexes

Hirosato Yamazaki, Akinori Shouji, Masashi Kajita, Masayuki Yagi*

Department of Materials Science and Technology, Faculty of Engineering, and Center for Transdisciplinary Research, Niigata University, 8050 Ikarashi-2, Niigata 950-2181, Japan

Contents

ARTICLE INFO

Article history:
Received 13 November 2009
Accepted 7 February 2010
Available online 12 February 2010

Keywords:
Artificial photosynthesis
Water oxidation catalyst
Photocatalyst
Electrocatalyst

ABSTRACT

The construction of an artificial photosynthetic device requires detailed understanding of the catalytic aspects of photo- or photoelectro-driven water oxidation. This has been attracting much interest as one of the promising clean energy-providing systems for the future. This review mainly covers progress on electrocatalytic and photocatalytic systems for water oxidation in the last decade. It includes conventional iridium oxide colloid catalysts and the new electrodeposited cobalt-phosphate catalyst films for water oxidation.

1. Introduction

Artificial photosynthetic devices have attracted much interest as future clean energy-providing systems [1–4]. Development of an efficient and robust catalyst for water oxidation to evolve O_2 (Eq. (1)) is a key task to yield a breakthrough for constructing an artificial photosynthetic device:

$$2H_2O \xrightarrow{\text{Water oxidation catalyst}} O_2 + 4H^+ + 4e^- \quad (1)$$

Much effort has been devoted to seek such a catalyst [4–8]. In the last decade, significant progress has been reported in the development of manganese, ruthenium and iridium complexes as water oxidation catalysts [8–10]. For a majority of the related studies, the molecular aspects of the catalysts have been studied to provide hints for development of an efficient catalyst, as well as to gain clues to reveal the mechanism of O_2 evolution catalyzed at the photosynthetic *oxygen evolving complex* (OEC) whose active site is known to consist of a tetramanganese-oxo cluster [11–17]. Chemical water oxidation using oxidant reagents such as a Ce^{IV} ion has been extensively studied in a homogenous system for most cases. Much attention should be paid into the catalytic aspect in photo- or photoelectro-driven water oxidation toward development of an artificial photosynthetic device. Recently, significant

* Corresponding author. Fax: +81 25 262 6790.
E-mail address: yagi@eng.niigata-u.ac.jp (M. Yagi).

0010-8545/$ – see front matter © 2010 Elsevier B.V. All rights reserved.
doi:10.1016/j.ccr.2010.02.008

advances have been made on electrocatalytic and photocatalytic water oxidation. This review will mainly cover the related progress in the last decade since the earlier reviews [4–6]. Our interest will be focused on the catalytic aspects of electrochemical and photochemical water oxidation in this review, though essential conclusions of redox chemistry and chemical water oxidation will be included to comprehensively understand the catalysis. The advanced extension of conventional iridium oxide colloid catalysts to electrochemical and photoelectrochemical systems was recently reported. Moreover, the new electrodeposited cobalt-phosphate catalysts were reported as an active and robust catalyst film for water oxidation [18–22]. Although iridium oxide colloid catalysts and cobalt-phosphate catalysts are not molecular catalysts, they are included in this review because they are promising materials based on metal coordination.

2. Catalytic aspects in the electrochemical and photochemical water oxidation

2.1. Manganese complex catalysts

2.1.1. $[(terpy)(H_2O)Mn(\mu\text{-}O)_2Mn(terpy)(H_2O)]^{3+}$ complex

Manganese complexes have made significant contributions to studies related to the structure and function of OEC in photosynthesis [4–8]. Water oxidation chemistry by synthetic manganese complexes has undoubtedly become of great interest since O_2 evolution by $[(terpy)(H_2O)Mn(\mu\text{-}O)_2Mn(terpy)(H_2O)]^{3+}$ (terpy = 2,2′:6′,2″-terpyridine) (Mn dimer) was reported nearly a decade ago [23,24].

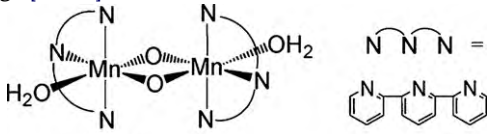

Mn dimer

The reaction of Mn dimer with an oxygen donor agent of sodium hypochlorite (NaClO) or potassium peroxymonosulfate ($KHSO_5$) in an aqueous solution led to O_2 evolution. The maximum turnover of Mn dimer for O_2 evolution was 4 for 6 h using NaClO, and the catalytic cycle was ended by decomposition of Mn dimer to permanganate ions [23]. They investigated water oxidation by Mn dimer in solution using a one-electron Ce^{IV} oxidant instead of the oxygen donor agents to relate the catalysis by Mn dimer to photosynthetic O_2 evolution at OEC where electron transfer is the source of oxidizing equivalents [25]. O_2 was detected in the reaction under the conditions of 250 μM Mn dimer and 30 mM Ce^{IV}, but the maximum turnover number (0.54) of Mn dimer was less than unity, showing non-catalytic O_2 evolution by Mn dimer with Ce^{IV}. The catalysis by Mn dimer in an aqueous solution using a Ce^{IV} oxidant was tested by another groups, but O_2 evolution was not observed [26,27] in disagreement with the earlier report [25]. This disagreement might be due to either the lower detection limit of the O_2 analysis or the different measurement conditions. These results show that the electron oxidant is not effective for water oxidation by Mn dimer because in the mechanism proposed for O_2 evolution using the oxygen donor agents ClO^- or HSO_5^-, an oxygen atom transfer from the oxygen donor agent to the manganese center of Mn dimer is involved as an initial reaction step [27]. Baffert et al. studied the electrochemical oxidation of Mn dimer in an aqueous electrolyte solution [28]. They concluded that Mn dimer cannot act as a homogeneous electrocatalyst for water oxidation due to formation of the inactive tetranuclear complex with a μ-oxo briged linear core structure from the Mn^{IV}–Mn^{IV} state of Mn dimer.

The reaction of Mn dimer with a Ce^{IV} oxidant catalytically produces O_2 from water when Mn dimer is adsorbed on layer compounds such as kaolin, mica and montmorillonite K10, though Mn dimer decomposes to MnO_4^- by its disproportionation without O_2 evolution in solution [26,29,30]. The maximum turnover numbers of Mn dimer adsorbed on mica and kaolin for O_2 evolution were 15 and 17 for 4 days catalysis, respectively, under optimum conditions. The kinetic analysis of O_2 evolution suggested that catalysis requires cooperation of two equivalents of Mn dimer adsorbed on layer compounds. The catalytic activity of Mn dimer induced by its adsorption onto the interlayer compounds was explained by either suppression of MnO_4^- formation competing with the catalysis or a high concentration of Mn dimer resulting in the close proximity between Mn dimers that is favorable for the cooperative catalysis on layer compounds. The Mn dimer/mica catalyst was extended to a photochemical system containing $[Ru(bpy)_3]^{2+}$ (bpy = 2,2′-bipyridine) and $S_2O_8^{2-}$ ions as a photosensitizer and a sacrificial electron acceptor, respectively [31]. $[Ru(bpy)_3]^{2+}$ was adsorbed onto the mica/Mn dimer adsorbate when the adsorbate is added in an aqueous $[Ru(bpy)_3]^{2+}$ solution, yielding a mica/Mn dimer/$[Ru(bpy)_3]^{2+}$ hybrid. Visible light irradiation (λ > 420 nm) to the suspension of the hybrid (10 mg mica, 1.6 μmol Mn dimer, 0.25 μmol $[Ru(bpy)_3]^{2+}$) in a 15 mM $Na_2S_2O_8$ aqueous solution produced 5.5 μmol of O_2 for 17 h. The turnover numbers of Mn dimer and $[Ru(bpy)_3]^{2+}$ were 3.4 and 88, respectively. Neither using mica/Mn dimer, mica/$[Ru(bpy)_3]^{2+}$ nor neat mica instead of the mica/Mn dimer/$[Ru(bpy)_3]^{2+}$ hybrid, was photochemical O_2 evolution observed. This shows that adsorption of both Mn dimer and $[Ru(bpy)_3]^{2+}$ on mica is important for photochemical O_2 evolution. Photochemical water oxidation experiment using ^{18}O-labeled water corroborated that the source of O_2 evolved is exclusively from bulk water. For photoluminescent measurement, photoexcited $[Ru(bpy)_3]^{2+}$ in mica was efficiently quenched by Mn dimer adsorbed, but not quenched by $S_2O_8^{2-}$ in a bulk aqueous solution at all, although it is efficiently quenched by the both in a homogeneous aqueous solution. The anionic mica layer matrix does not allow $S_2O_8^{2-}$ anions to go into the interspace between mica layers for quenching of photoexcited $[Ru(bpy)_3]^{2+}$. For the presumed mechanism of photochemical water oxidation, photoexcited $[Ru(bpy)_3]^{2+}$ in mica is reductively quenched by Mn dimer adsorbed to form the oxidized Mn dimer (not identified yet) and $[Ru(bpy)_3]^{+}$, and the latter is scavenged by $S_2O_8^{2-}$ to regenerate the ground state of $[Ru(bpy)_3]^{2+}$. Two equivalents of the oxidized Mn dimer could cooperatively catalyze water oxidation, as seen in a chemical water oxidation system using a Ce^{IV} oxidant. This is supported by the second order kinetics of photochemical O_2 evolution rate with respect to Mn dimer adsorbed. The photochemical water oxidation by the mica/Mn dimer/$[Ru(bpy)_3]^{2+}$ hybrid can be regarded as a PSII model reaction, where Mn dimer and $[Ru(bpy)_3]^{2+}$ act the roles of OEC comprised of manganese-oxo cluster and a chlorophyll photoexcitation center (P_{680}) in PSII, respectively.

2.1.2. Mn_4O_4 cubane complexes

The synthesis and characterization of a tetramanganese complex, $L_6Mn_4O_4$ (L^- = diphenylphosphinate), with Mn_4O_4 ($2Mn^{III}$, $2Mn^{IV}$) cubane core were reported [32]. The observed reaction pathways of $L_6Mn_4O_4$ are shown in Fig. 1. $L_6Mn_4O_4$ reacted with the hydrogen atom donor, phenothiazine in a CH_2Cl_2 solution, forming $L_6Mn_4O_2$ and $[L_5Mn_4O_2]^+$ as well as releasing two water molecules from the core [33]. This result shows that two of the corner oxo atoms of the cubane can be converted into two labile water molecules. It was also found that UV light absorption by $L_6Mn_4O_4$ converts two of the corner oxos of the cubane into an O_2 molecule, which is released only if one of the bridging chelates is also released to form $[L_5Mn_4O_2]^+$ selectively [34,35]. The O_2 evolution from the Mn_4O_4 cubane core was corroborated by the detection of $^{18}O_2$ from $L_6Mn_4(^{18}O)_4$. By contrast, other manganese-oxo core types, including $Mn^{III}(\mu\text{-}O)_2Mn^{IV}$, undergo non-selective photo-destruction of the complexes without O_2 production [35].

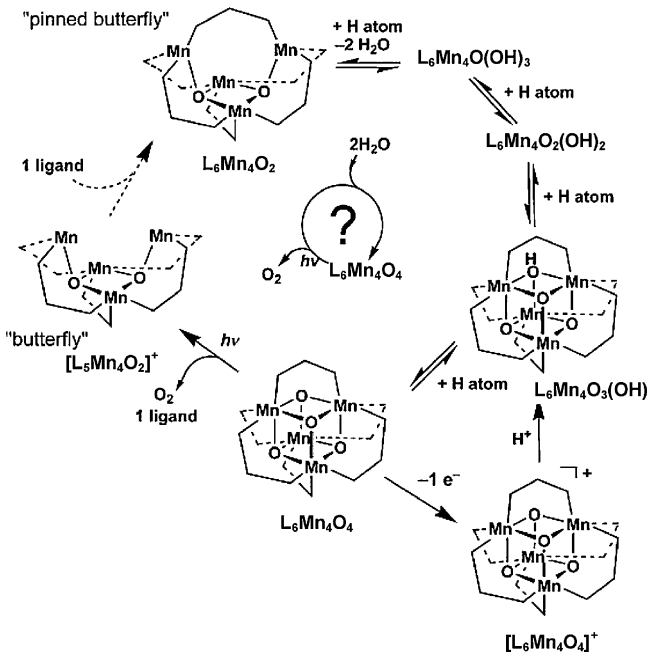

Fig. 1. Reaction pathways and possible photocatalytic cycle for the manganese-oxo cubane, $L_6Mn_4O_4$, L = diphenylphosphinate ($Ph_2PO_2^-$) or bis(4-methoxyphenyl)phosphinate ($(4\text{-MeOPh})_2PO_2^-$). Reaction pathways include observed reduction reactions of $L_6Mn_4O_4$ and $[L_6Mn_4O_4]^+$ in solution and gas-phase photodissociation to yield O_2. (Reprinted with permission from [36]. Copyright © 2008 WILEY-VCH Verlag GmbH & Co. KGaA.)

The Mn_4O_4 cubane geometry exhibits unique reactivity in O_2 evolution. It was suggested that intramolecular O–O bond coupling of the oxo bridges for production of O_2 is possible in complexes containing the longer Mn-O(μ_3-oxo) bonds (1.95 Å) of the cubane core than that (1.8 Å) observed for $Mn^{III}(\mu\text{-O})_2Mn^{IV}$ cores. The Mn_4O_4 cubane core is a reactive intermediate for the chemical transformation of the oxo bridges to both water and O_2. This observation suggests the possibility of creating a catalytic cycle (Fig. 1) that could oxidize two water molecules bound to $L_6Mn_4O_2$ along the reverse reaction of the release of water from the $L_6Mn_4O_4$ cubane core, eventually releasing O_2 from the core involving photodissociation of a phosphate chelate ligand. However, it has not proved possible to realize a catalytic cycle in Fig. 1, because O_2 is not photoreleased form $\{Mn_4O_4\}^{6+}$ or $\{Mn_4O_4\}^{7+}$ cubane core in a condensed phase [34]. Recently, catalytic water oxidation by a cubane complex was established in a photoelectrochemical system where a new cubane derivative with $L'^- =$ bis(4-methoxylphenyl)phosphinate is confined in a Nafion membrane that comprises hydrophobic fluorocarbon domains separated by hydrophilic sulfonic groups forming an aqueous channel for cations [36–40]. One-electron-oxidized cubane complex $[L'_6Mn_4O_4]^+$ (cubane) was incorporated into the Nafion coated on a glassy carbon electrode from its acetonitrile solution by cation exchange. Photoanodic current was induced by light irradiation (275–750 nm, 150 mW cm^{-2}) from a filtered Xe light source to the cubane/Nafion/glassy carbon electrode (3 mm diameter) polarized at 1.0 V (vs. Ag/AgCl) in an aqueous 0.1 M Na_2SO_4 solution. It slowly degrades to approximately 75% of the initial current in 65 h. H^+ and O_2 were identified as products in the photoelectrocatalysis by the measured pH and O_2 concentration in the electrolyte solution. The turnover number of the cubane complex was approximately 1000 during the 65 h catalysis based on net charge (0.163 C) and the coverage (0.27 nmol) of the cubane complex. The photoelectrocatalysis experiment in an ^{18}O-labeled water medium corroborated that the oxygen atom source of O_2 evolved is bulk water. 1.31 μmol of O_2 was evolved using a cubane/Nafion/Pt plate electrode (10 mm × 15 mm) held at 1.0 V (vs. Ag/AgCl) during illumination with filtered Xe light (7.5 h, 100 mW cm^{-2}). The charge passed during the photoelectrocatalysis was 0.49 C, corresponding to 97% of Faraday efficiency. It was postulated that the aqueous cubane/Nafion/electrode system exhibits the same photoreaction as seen for cubane in the gas-phase [41], with O_2 being released only upon photodissociation of a phosphinate ligand L'^- to yield "reduced butterfly" $[L'_5Mn_4O_2]^{2+}$. This species is known to slowly polymerize if formed in organic solvents [33], but appears to be more stable in the restricted hydrophobic pocket of Nafion. Water is known to bind to manganese ions in a reduced butterfly complex that forms reductively in solution [33]. The mechanism of the oxidative branch in the catalytic cycle in Nafion was presumed to be light-independent electrooxidation of $[L'_5Mn_4O_2]^{2+}$ involving L'^- and two molecules of water to reform cubane. However, the active species and mechanism of the catalysis remain to be fully elucidated. The requirement of light implies that there is an additional limiting reaction required for catalyst activation, which effectively contributes to a larger over potential. Photo-activation of the cubane catalyst due to photodissociation of a chelate phosphonate ligand could give a new concept for design of water oxidation catalyst. Immobilization of a water-insoluble catalyst onto an interface between hydrophobic domain and a hydrophilic aqueous ions channel in Nafion could be important for stable catalysis. The stabilization of water-soluble catalyst by immobilization into a Nafion membrane is well-established for ruthenium ammine complex/Nafion systems [42–48].

2.2. Ruthenium complex catalysts

2.2.1. $Ru^{III}(\mu\text{-O})Ru^{III}$ complexes

The trail blazing ruthenium-based catalyst, $[(bpy)_2(H_2O)Ru^{III}(\mu\text{-O})Ru^{III}(H_2O)(bpy)_2]^{4+}$ with a $Ru^{III}(\mu\text{-O})Ru^{III}$ core, so-called blue dimer, was reported by Meyer et al. in the early 1980s [49–51]; its derivatives are also found to be active catalysts [52,53]. The turnover frequency and turnover number of blue dimer were reported to be 4.2×10^{-3} s^{-1} [54] and 13.2 [55], respectively. Although a large number of studies have been reported on the structure, redox properties and the catalytic aspect of blue dimer, a consensus on the mechanism of water oxidation catalyzed by blue dimer has not yet been established [49–63]. The μ-oxo ruthenium(II) dimer derivative modified with phosphonate groups, $[(PO_3H_2\text{-terpy})(H_2O)_2Ru^{III}(\mu\text{-O})Ru^{III}(H_2O)_2(PO_3H_2\text{-terpy})]^{4+}$ (PO_3H_2-terpy = 4′-phosphonato-2,2′:6′,2″-terpyridine) was synthesized to extend the μ-oxo dimer-based water oxidation chemistry to metal oxide surfaces such as ZrO_2, TiO_2, or SnO_2 [64]. The phosphonate linkers are more effective to attach the complex stably on the metal oxide surface in an aqueous medium than carboxylate linkers. The CV of the phosphonate-modified complex exhibits successive redox waves from Ru^{II}-O-Ru^{II} to Ru^{V}-O-Ru^{VI}, including a 2-electron process of Ru^{II}-O-Ru^{II}/Ru^{III}-O-Ru^{III} and a proton-coupled redox reaction of Ru^{III}-O-Ru^{III}/Ru^{III}-O-Ru^{IV}. The electrocatalytic water oxidation by the phosphonate-modified complex adsorbed on ZrO_2 films on fluorine-doped tin oxide (FTO) was carried out at applying 1.5 or 1.25 V (vs. Ag/AgCl) at pH = 1 and 1.32 or 1.15 V at pH = 6. (The former and latter potentials are for Ru^{V}-O-Ru^{VI} and Ru^{V}-O-Ru^{V} formation, respectively for both the pH.) The catalytic currents fell to ∼10% of their initial value within 30 min and 1 h for Ru^{V}-O-Ru^{V} and Ru^{V}-O-Ru^{VI}, respectively. Turnover numbers of the complex are 1.8 (pH = 1) and 3.0 (pH = 6) for Ru^{V}-O-Ru^{VI} and ∼1 (pH = 1) and 2.6 (pH = 6) for Ru^{V}-O-Ru^{V}. It was thus demonstrated that single electron transfer activation of multiple electron transfer and water oxidation can be transferred to the electrode interface surface on oxide electrodes. However, the extent of catalytic activity is limited, and the author pointed out the importance of

the evolution of related, robust family of surface-bound catalysts for water oxidation [64].

2.2.2. Dinuclear ruthenium complexes chelated by polypyridyl multi-dentate ligands

In the recent past, several dinuclear ruthenium complexes chelated by polypyridyl multi-dentate ligands have been reported [65–68]. A dinuclear ruthenium complex, $[(terpy)(H_2O)Ru^{II}(bpp)Ru^{II}(H_2O)(terpy)]^{3+}$ bridged by a bpp^- (3,5-bis(2-pyridyl)pyrazolate) chelating ligand was reported as an active catalyst for water oxidation by Sens et al. [65]. Zong and Thummel synthesized another dinuclear ruthenium complex ($[Ru_2(macroN_6)(Rpy)_4Cl]^{3+}$) in which two ruthenium(II) ions are chelated by an equatorial bis-tridentate ligand, 3,6-bis-[6′-(1″,8″-naphthyrid-2″-yl)-pyrid-2′-yl]pyridazine ($macroN_6$) and a chloro ligand and the axial coordination sites of each ruthenium center are occupied by four alkyl pyridine (Rpy) ligands [66]. However, electrocatalysis and photocatalysis by these new families of ruthenium dimer catalysts have not yet been reported.

The dinuclear ruthenium complex, $[(tBu_2qui)(OH)Ru^{II}(btpyan)Ru^{II}(OH)(tBu_2qui)]^{2+}$ with 3,6-di-*tert*-butyl-1,2-benzoquinone (tBu_2qui) ligands on each metal center and a bridging ligand of 1,8-bis(2,2′:6′,2″-terpyridyl)anthracene was synthesized [67,68] (see illustration [69]).

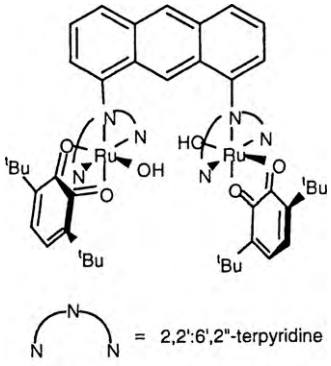

Ru btpyan complex

The key concept for the btpyan dimer is the pool of oxidizing equivalents on redox active ligands in addition to the ruthenium centers for water oxidation. The addition of 2 eq of potassium *tert*-butoxide (*t*BuOK) to the btpyan dimer solution in methanol caused the reduction of tBu_2qui ligands by intramolecular electron transfer from the hydroxo ligands to quinone ligands coupled with proton dissociation of hydroxo ligands, resulting in $[(tBu_2sq)(O)Ru^{II}(btpyan)Ru^{II}(O)(tBu_2sq)]^0$ (tBu_2sq = 3,6-di-*tert*-butyl-1,2-semiquinone) (Eq. (2)). The oxo ligand formed on each center was hypothesized to be a radical with the possibility to form a peroxo O–O bond by intramolecular coupling of the oxo ligand:

$$[(tBu_2qui)(OH)Ru^{II}(btpyan)Ru^{II}(OH)(tBu_2qui)]^{2+} \underset{2H^+}{\overset{-2H^+}{\rightleftarrows}} [(tBu_2sq)(O)Ru^{II}(btpyan)Ru^{II}(O)(tBu_2sq)]^0 \quad (2)$$

The resultant complex $[(tBu_2sq)(O)Ru^{II}(btpyan)Ru^{II}(O)(tBu_2sq)]^0$ underwent ligand-localized oxidation at 0.4 V (vs. Ag/AgCl) in methanol to give $[(tBu_2qui)(O)Ru^{II}(btpyan)Ru^{II}(O)(tBu_2qui)]^{2+}$. The latter further underwent metal-localized oxidation at 1.2 V in CF_3CH_2OH/ether to yield $[(tBu_2qui)(O)Ru^{III}(btpyan)Ru^{III}(O)(tBu_2qui)]^{4+}$, which presumably catalyzes water oxidation (Eq. (3)):

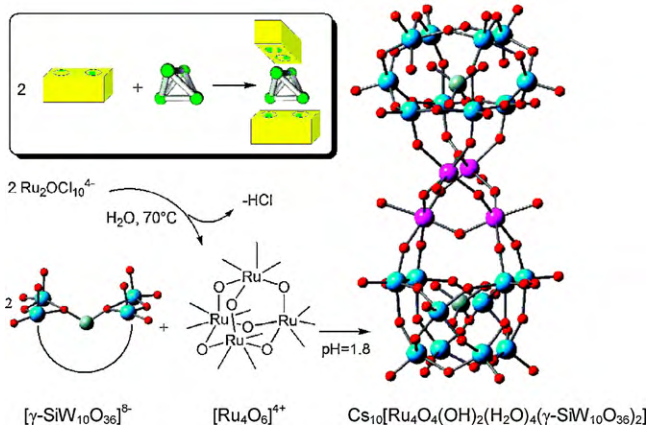

Fig. 2. Formation scheme of the polyoxometalate Ru_4 complex, di-γ-decatangstsilicate embedding a tetra-ruthenium(IV)-oxo core, $Cs_{10}[Ru_4O_4(OH)_2(H_2O)_4(\gamma\text{-}SiW_{10}O_{36})_2]$. (Reprinted with permission from [70]. Copyright 2008 American chemical Society.)

$$[(tBu_2sq)(O)Ru^{II}(btpyan)Ru^{II}(O)(tBu_2sq)]^0 \underset{2e^-}{\overset{-2e^-}{\rightleftarrows}} [(tBu_2qui)(O)Ru^{II}(btpyan)Ru^{II}(O)(tBu_2qui)]^{2+} \underset{1.2\,V}{\overset{-2e^-}{\rightleftarrows}} [(tBu_2qui)(O)Ru^{III}(btpyan)Ru^{III}(O)(tBu_2qui)]^{4+} \quad (3)$$

The potentiostatic electrolysis at 1.7 V vs. Ag/AgCl evolved 15.2 ml (turnover number of the btpyan dimer: 33,500) of O_2 for 40 h using a btpyan dimer-coated ITO electrode (2.0×10^{-8} mol per 10.0 cm^2) dipped in an aqueous buffer solution (pH 4.0, H_3PO_4/KOH, 1.0 M), showing that the btpyan dimer can work as a stable electrocatalyst for water oxidation [68].

2.2.3. Tetra-ruthenium complex with all inorganic ligands

Recently, the polyoxometalate Ru_4 complex, di-γ-decatungstsilicate embedding a tetra-ruthenium(IV)-oxo core was isolated by a reaction of divacant polyoxometalate, $[\gamma\text{-}SiW_{10}O_{36}]^{8-}$ with μ-oxo-bis-pentachlororuthenate(IV), $Ru_2OCl_{10}^{4-}$ in an aqueous solution (Fig. 2) [70]. The X-ray diffraction-derived structure was reported from two different groups [70,71]. The polyoxometalate Ru_4 complex works as a homogeneous catalyst for water oxidation in chemical water oxidation systems using a Ce(IV) [70] or $[Ru(bpy)_3]^{3+}$ [71] oxidant. In the Ce(IV)-oxidation system, O_2 was evolved in the reaction of 4.3 μmol of the Ru_4 catalyst with 1720 μmol of Ce(IV) in water at pH = 0.6 and 20 °C, and the O_2 evolution was saturated in 2 h [70]. The amount of O_2 evolved for the catalysis is 385 μmol, corresponding to 90% yield based on the added Ce(IV) oxidant. The turnover number of the Ru_4 catalyst was 90 under the conditions employed. Linear dependence of the initial rate on the Ru_4 catalyst concentration was given, with a pseudo-first order kinetic constant of 9.92×10^{-3} s^{-1} (0.045–1.45 μmol catalyst, 10.9 mmol Ce(IV)). The integrity of the catalyst structure after treatment of Ce(IV) excess was confirmed by infra red and resonance Raman spectroscopic techniques. In the $[Ru(bpy)_3]^{3+}$-oxidation system, the reaction between the Ru_4 catalyst and $[Ru(bpy)_3]^{3+}$ was followed by monitoring formation of $[Ru(bpy)_3]^{2+}$ in a UV–visible absorption spectroscopic technique as well as monitoring the amount of O_2 in the headspace of the reaction vessel using the gas chromatography (GC) technique [71]. The aqueous solution containing 1.2 mM (12 μmol) $[Ru(bpy)_3]^{3+}$ and 10 μM (0.1 μmol) Ru_4 catalyst gave 10.7 μmol $[Ru(bpy)_3]^{2+}$

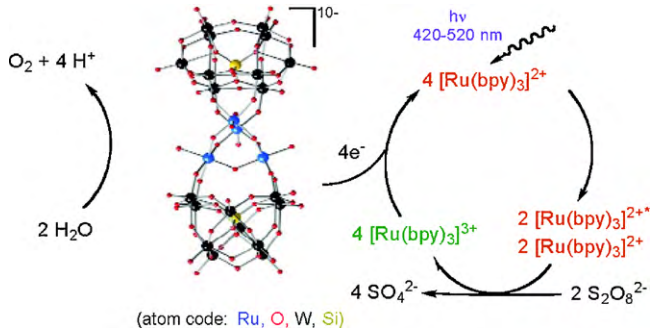

Fig. 3. Reaction scheme of light-driven catalytic water oxidation by the polyoxometalate Ru_4 complex using $[Ru(bpy)_3]^{2+}$ and $S_2O_8^{2-}$ ions as a photosensitizer and a sacrificial electron acceptor, respectively. (Reprinted with permission from [72] Copyright 2009 American chemical Society.)

and 1.78 μmol O_2. The yields of the $[Ru(bpy)_3]^{2+}$ formed and O_2 were 90% and 60% based on initial $[Ru(bpy)_3]^{3+}$, respectively. The turnover number of the Ru_4 catalyst was 18 under the conditions employed. The light-driven water oxidation by the Ru_4 catalyst was reported in a $[Ru(bpy)_3]^{2+}$ photosensitizer/$S_2O_8^{2-}$ sacrificial electron acceptor system [72] (Fig. 3). The photochemical reaction in an 20 mM sodium phosphate buffer solution (8 mL) containing 1.0 mM $[Ru(bpy)_3]^{2+}$, 5 mM $Na_2S_2O_8$ and 5.0 μM Ru_4 catalyst with a filtered Xe light source (420–520 nm, 28 mW cm^{-2}) was followed by monitoring both the concentration of $Na_2S_2O_8$ consumed and O_2 evolved. 7.2 μmol of O_2 was evolved with 38 μmol of $Na_2S_2O_8$ consumed during 35 min catalysis. The O_2 yield per two equivalents of $Na_2S_2O_8$ was 38%. The turnover number of the Ru_4 catalyst was 180 with the initial turnover frequency of 8×10^{-2} s^{-1}. The authors pointed out that the quantum efficiencies for generating $[Ru(bpy)_3]^{3+}$ (44%) and its reaction with the Ru_4 catalyst to form O_2 (60%) are major limiting factors in this system and that the overall quantum efficiency can be improved with a better scheme for generating $[Ru(bpy)_3]^{3+}$.

2.2.4. Mononuclear ruthenium(II) pincer complex

A solution-phase reaction scheme was reported in which H_2 and O_2 evolve in consecutive thermal- and light-driven steps mediated by well-defined mononuclear ruthenium(II) pincer complexes, respectively [73] (Fig. 4). The reaction of a de-aromatized hydride Ru(II) pincer complex (hydride complex, see Fig. 4) with water at 25 °C yields a *trans* hydride-hydroxo Ru(II) complex that was characterized by NMR spectra and X-ray diffraction analysis. Heating the *trans* hydride-hydroxo complex in refluxing water for 3 days resulted in evolution of H_2 (37% yield by GC) with concomitant formation of the *cis* dihydroxo complex (45% yield by NMR). Irradiation of the *cis* dihydroxo complex in THF or water under N_2 or Ar with filtered halogen lamp (300 W, λ > 320 nm) over 2 days resulted in a color change from green to greenish yellow, accompanied by O_2 evolution (23% yield by GC-MS). The NMR data of the solution showed that the *trans* hydride-hydroxo complex (45% yield) was formed in addition to the unreacted *cis* dihydroxo complex (33% yield) and unidentified by-products (22% yield). Irradiation of the *cis* dihydroxo complex in water under the Ar flow conditions to remove the generated O_2 resulted in clean conversion of the *cis* dihydroxo complex to the hydride-hydroxo complex (49% yield, the rest being the unreacted complex) without by-products. Upon irradiation of an ^{18}O-labeled dihydroxo complex (dihydroxo-$^{18}O^{18}O$) with two ^{18}OH groups in H_2O, $^{36}O_2$ was formed as the major dioxygen product, as measured by GC-MS. No exchange of an O atom between dihydroxo-$^{18}O^{18}O$ and H_2O was confirmed. These results verify that O_2 was released from two hydroxo groups. Isotropically mixed-labeled dihydroxo complex (dihydroxo-$^{18}O^{16}O$) was prepared, and irradiation of dihydroxo-$^{18}O^{16}O$ in H_2O generated $^{34}O_2$ predominantly with only small amounts of $^{32}O_2$ and $^{36}O_2$. Contrastingly, $^{32}O_2$ and $^{36}O_2$ were generated with only small amount of $^{34}O_2$ in photolysis involving equimolar amounts of dihydroxo-$^{18}O^{18}O$ and abundant dihydroxo-$^{16}O^{16}O$ complexes. These results show that the O–O bond formation is an intramolecular process on a single metal center. The author suggested that on photolysis, the dihydroxo complex liberates hydrogen peroxide in a reductive elimination step, which catalytically disproportionates into O_2 and water. The stepwise catalytic cycle to split water to H_2 and O_2 can be provided by combining the separate processes of thermal H_2 evolution (in refluxing water) from the *trans* hydrido hydroxo complex to yield the *cis* dihydroxo complex and light-driven O_2 evolution from the dihydroxo complex to yield the *trans* hydrido hydroxo complex.

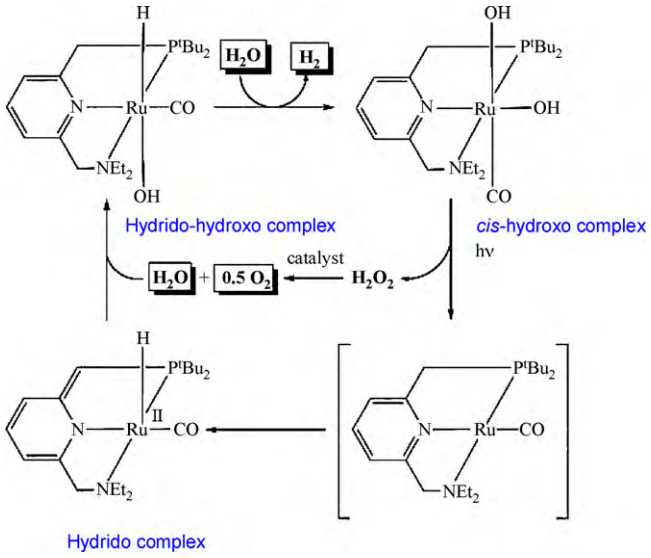

Fig. 4. Proposed mechanism for consecutive H_2 and O_2 evolution by a mononuclear ruthenium (II) pincer complex. (Reprinted with permission from [73]. Copyright 2009 by the American Association for the Advancement of Science.)

2.3. Iridium oxide colloid catalysts

It is well-known that metal oxides such as RuO_2, IrO_2, PtO_2, Co_3O_4, and Rh_2O_3 have catalytic activities for water oxidation [74–78]. RuO_2, an efficient catalyst, has been well-studied as a colloidal and as a heterogeneous catalysts in electrochemical and photochemical systems [75,76], although RuO_2 is easily converted to unstable RuO_4 [79]. IrO_2 has comparative activity to RuO_2 and is more stable than the latter [54,74]. Harriman and Thomas prepared stable IrO_2 colloid stabilized by citrate ions using a simple and easy technique [80]. IrO_2 colloid has been utilized as an efficient catalyst for photochemical water oxidation in a homogeneous system containing a $[Ru(bpy)_3]^{2+}$ photosensitizer and a $S_2O_8^{2-}$ electron acceptor [81–83]. However, the catalytic activity of IrO_2 colloid was not reported although the turnover numbers of $[Ru(bpy)_3]^{2+}$ photosensitizer were reported.

Recently, IrO_2 colloid stabilized by citrate ions was self-assembled onto an ITO electrode to form a monolayer of the colloidal IrO_2 particles when the ITO is immersed in the colloid solution at pH = 3.5 [84,85] (Fig. 5). The self-assembly was promoted steeply at pH = 3.5–4.1 although it hardly occurs at pH = 5.3–9.7. It is supposed to be caused by chemical interaction between carboxylic groups of the citrate stabilizer and hydroxyl groups of the ITO surface. The adsorption isotherm of IrO_2 colloid onto the ITO surface was analyzed by the Langmuir adsorption isotherm to provide the

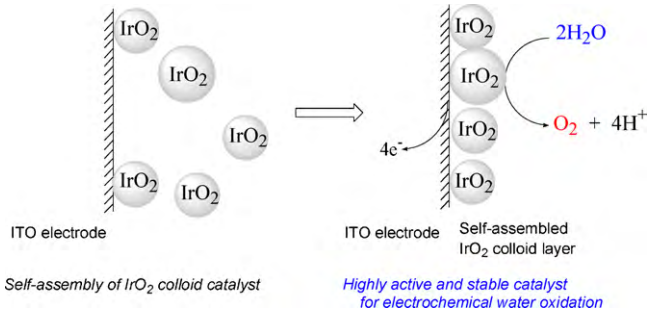

Fig. 5. Imaged illustrations of self-assembly of citrate-stabilized IrO_2 colloid and electrochemical water oxidation at an IrO_2 colloid layer.

maximum coverage and the adsorption equilibrium constant as 1.1×10^{-8} mol cm^{-2} (based on Ir site) and 1.8×10^{4} M^{-1} at 25 °C, respectively. In electrocatalytic water oxidation at 1.3 V vs. Ag/AgCl for 1 h using the IrO_2 colloid-assembled ITO electrode, the steady anodic current density (0.88 mA cm^{-2}) at 1 h was higher than that (0.46 μA cm^{-2}) of a bare ITO electrode by three orders of magnitude, and the amount of O_2 evolved during the electrocatalysis was 7.6 μmol cm^{-2} h^{-1}. The amount of O_2 evolved increased linearly with the coverage of IrO_2 in the range of 0.60–6.8 $\times 10^{-10}$ mol cm^{-2}, meaning that the catalytic activity of IrO_2 colloid does not depend on the amount of IrO_2 colloid adsorbed on the electrode. The turnover frequency of IrO_2 colloid was 23,600 h^{-1} (based on Ir site) from the slope.

A tri-nuclear ruthenium complex ($[(NH_3)_5Ru\text{-}O\text{-}Ru(NH_3)_4\text{-}O\text{-}Ru(NH_3)_5]^{6+}$) works efficiently for electrocatalytic water oxidation when it is adsorbed on a platinum black electrode, with turnover frequency 1500 h^{-1} at 1.3 V vs. Ag/AgCl [86]. The turnover frequency of IrO_2 electrodeposited on the ITO electrode was 12,700–16,400 h^{-1} at 1.3 V vs. Ag/AgCl [87]. The turnover frequency (23,600 h^{-1}) is higher than those hitherto-reported catalysts for electrochemical water oxidation.

IrO_x nanoparticles (1.6 ± 0.6 nm diameter) capped solely by hydroxide were prepared by thermal hydrolysis of K_2IrCl_6 at pH = 13 without addition of stabilizer ligands. Homogeneous electrocatalysis was performed for water oxidation by electroactive IrO_x nanoparticles dissolved in an alkaline solution (pH = 13) [88]. In rotating ring disk electrode experiments, the mass transport-controlled plateau of the nanoparticle $Ir^{V/IV}$ wave at 0.45 V vs. Ag/AgCl was observed followed by the catalytic current with 100% Faraday efficiency at 0.55 V (an overpotential of 0.29 V) for water oxidation reflecting electrochemical generation of Ir^{VI} states. The Ir site turnover frequency was 8–11 s^{-1}. Controlled potential coulometry showed that all Ir sites in these nanoparticles are electroactive, meaning that the nanoparticles are small enough to allow the required electron and proton transport throughout. IrO_x nanoparticles capped by hydroxide were electro-flocculated on a glassy carbon electrode at 1.3 V vs. Ag/AgCl to form stable, adherent, mesoporous films of IrO_x nanoparticles [89]. These films initiate O_2 evolution from water oxidation and then achieve 100% current efficiency at overpotentials of 0.25 V defined as the potential giving 0.5 mA cm^{-2} of a catalytic current density. The turnover frequency of the electroactive Ir sites was estimated as 6.0 and 4.5 s^{-1} under the Ir coverage conditions of $<2 \times 10^{-9}$ and $\sim 6 \times 10^{-8}$ mol cm^{-2}, respectively. These values are slightly lower than those (8–11 s^{-1}) for homogeneous electrocatalysis.

Efficient charge separation is well-known to be induced by visible light at liquid junctions of dye-adsorbing n-type metal oxide semiconductors such as TiO_2, SnO_2 and ZnO_2, as studied actively for dye-sensitized solar cells [90,91]. The use of the efficient charge separation at liquid junctions is one of the promising approaches for photochemical water oxidation without an external sacrificial electron acceptor such as $S_2O_8^{2-}$, $[Co(NH_3)_5Cl]^{2+}$ and Ag^+. Recently, photochemical water oxidation based on the dye-photosensitization at a TiO_2 liquid junction was reported [92] (Fig. 6). The heteroleptic Ru dye was synthesized to serve as both a sensitizer component and molecular bridge to connect an IrO_2 colloid catalyst to a TiO_2 surface. The phosphonate groups are chemically selective for the TiO_2 surface and the malonate group is selective for the IrO_2 colloid surface. The bpy ligands in this complex minimize the distance between the ruthenium center and the surface of respective oxides. The photoelectrochemical cell was equipped with a nanoporous TiO_2 electrode adsorbing the IrO_2 colloid-attached Ru dye as a working electrode, and an Ag/AgCl reference electrode and a Pt wire counter electrode, immersed in a buffer solution of 30 mM Na_2SiF_6 (pH = 5.75 with $NaHCO_3$) containing 500 mM Na_2SO_4. Visible light irradiation (λ > 410 nm) on the working electrode at potentials positive of −325 mV vs. Ag/AgCl produced a measurable photoanodic current generating a spike in current which decayed rapidly, followed by a steady current (typically 10–30 μA cm^{-2}). Monochromic light irradiation at 450 nm (7.8 mW cm^{-2}) to the working electrode gave 12.7 μA cm^{-2} of a photoanodic current, corresponding to 0.9% of an internal quantum yield. The low quantum yield was likely due to slow electron transfer from the IrO_2 nanoparticles to the oxidized dye that does not compete efficiently with back electron transfer from a TiO_2

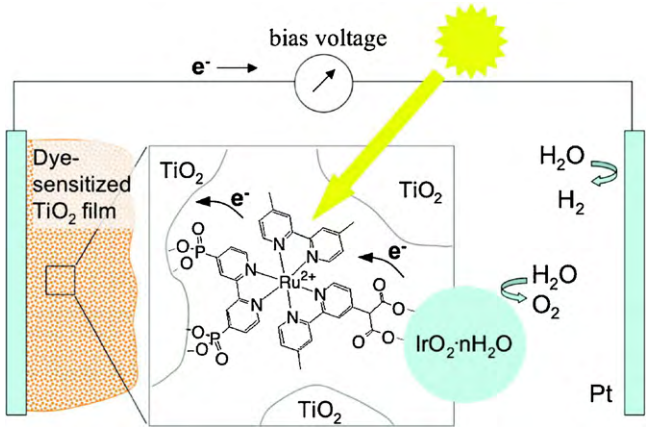

Fig. 6. Schematic illustration of photoassisted water splitting based on a dye-sensitized solar cell. (Reprinted with permission from [92]. Copyright 2009 American chemical Society.)

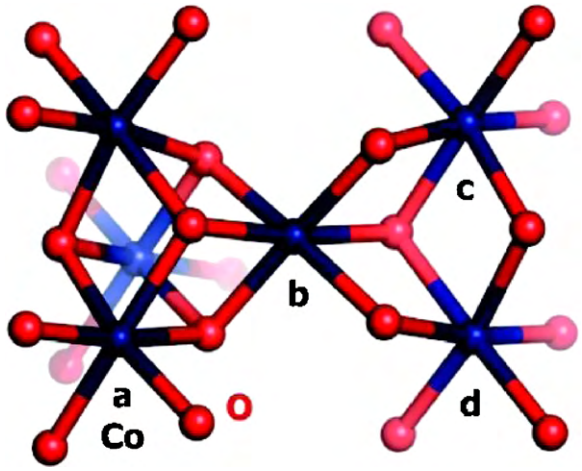

Fig. 7. Proposed structural motif deduced from XAS data relating to the bulk of the Co catalyst film (cobalt in blue, oxygen in red). (Reprinted with permission from [22]. Copyright 2009 American chemical Society.)

Table 1
Summery of turnover frequency (TOF), turnover number (TN) and marked features of the catalyst in electrochemical and photochemical water oxidation.

Catalysts		Systems[a]	TOF	TN	Conditions	Marked features	Refs.
Mn dimer complex	Homo. Electrochem.	Aqueous medium	–	–		No O_2 evolution, formation of tetranuclear Mn complex	[28]
	Homo. Photochem.	$[Ru(bpy)_3]^{2+}/S_2O_8^{2-}$ system	–	–		No O_2 evolution	[28]
	Hetero. Photochem.	Mica/Mn dimer catalyst, $[Ru(bpy)_3]^{2+}/S_2O_8^{2-}$ system, aqueous medium (pH =6.2)	1.1×10^{-4} s^{-1}	3.4	UV cut filtered halogen lamp (>420 nm, 127 mW cm^{-2}), 17 h catalysis		[31]
Mn_4O_4 cubane complex	Hetero. Photoelectrochem.	Electrode coated by Nafion film confining $Mn_4O_4^+$ cubane complex, aqueous medium		1,000	1.0 V vs. Ag/AgCl, Filtered Xe lamp, 65 h catalysis		[36]
Ru btpyan complex	Hetero. Electrochem.	Solid Ru btpyan complex-coating electrode, aqueous medium (pH = 4.0)		33,500	1.7 V vs. Ag/AgCl, 40 h catalysis, in aqueous medium		[68]
Ru_4 complex	Homo. Photochem.	$[Ru(bpy)_3]^{2+}/S_2O_8^{2-}$ system, aqueous medium (pH = 7.2)	8×10^{-2} s^{-1}	180	Filtered Xe lamp (420–520 nm, 28 mW cm^{-2}), 35 min catalysis		[72]
Ru pincer complex	Homo. Photochem.	THF or aqueous medium	–	–		Halogen lamp filtered through perspex, 22% yield of O_2 evolved during 2 days catalysis, undescribed catalytic reactions	[73]
IrO_2 colloid (citrate-stabilized)	Hetero. Electrochem.	Self assembled IrO_2 colloid on ITO or FTO electrode, aqueous medium (pH = 5.3)	23,600 h^{-1} (per Ir site)		1.3 V vs. Ag/AgCl, 1 h catalysis		[85]
IrO_x colloid (hydroxide-capped)	Homo. Electrochem.	Electro-flocculated IrO_x colloid on a electrode, aqueous medium (pH = 7.0)	4.5–6.0 s^{-1} (per Ir site)		Overpotential of 0.25 V vs. Ag/AgCl	100% of Faraday efficiency for O_2 evolution	[88]
	Hetero. Electrochem.	Aqueous medium (pH = 13)	8–11 s^{-1}		0.55 V vs. Ag/AgCl (overpotential of 0.29 V)	100% of Faraday efficiency for O_2 evolution	[89]
IrO_2 colloid (heteroleptic Ru dye-attached)	Hetero. Photoelectrochem.	Aqueous medium (pH = 5.75)	10–30 μA cm^{-2}		Visible light (>410 nm) 0 V vs. Ag/AgCl	20% of Faraday efficiency for O_2 evolution (450 nm monochromic light, 7.8 mW cm^{-2})	[92]
Co-P film catalysts	Hetero. Electrochem.	Aqueous medium (pH = 7.0)	>1 mA cm^{-2}		1.29 V vs. NHE	100% of Faraday efficiency for O_2 evolution	[19]

[a] "Homo." and "hetero." mean homogeneous and heterogeneous systems, respectively. "Electrochem.", "photoelectrochem." and "photochem." mean electrochemical, photoelectrochemical and photochemical systems, respectively.

conduction band to the oxidized dye. O_2 and H_2 evolution were confirmed by gas chromatography, and the Faraday efficiency for O_2 evolution was roughly 20% as measured by a pseudo-Clark electrode. However, the amount and Faraday efficiency of H_2 evolved were not indicated though they are important for confirmation of desired water splitting. The turnover number of the dye molecule was 16 for a 4 h-photochemical reaction. The nucleophilic attack on the oxidized dye causes the photocurrent to decay, as it is known to compete with water oxidation in a photosystem containing a $[Ru(bpy)_3]^{2+}$ derivative sensitizer and a sacrificial electron acceptor. This work undoubtedly illustrates a thoughtful design of an artificial photosynthetic device utilizing liquid junctions of dye-adsorbing semiconductors, and indicates difficulty in electron transfer between a catalyst and a dye sensitizer. This also might imply a substantive issue on electron transfer from a catalytic site to a dye molecule, attached on a colloid surface, is a dye molecule-attaching colloid catalyst system.

2.4. Cobalt catalyst

Recently, it was found that electrolysis of Co^{2+} ions in phosphate derivative buffer solutions allows the electrodeposition of a highly active water oxidation catalyst film on an ITO or FTO electrode [19,20]. The CV of 0.5 mM $Co(NO_3)_2$ in a 0.1 M phosphate buffer solution (pH = 7) exhibited an oxidative wave at 1.13 V vs. normal hydrogen electrode (NHE), followed by the onset of a strong catalytic wave at 1.23 V. The potentiostatic electrolysis at 1.29 V in the electrolyte solution employed, exhibited a rising current density that reaches a peak value more than 1 mA cm^{-2} after 8 h, accompanying film formation on the ITO electrode with effervescence given on the film. The amount of charge passed during the course of an 8 h electrolysis far exceeds what could be accounted for by stoichiometric oxidation of the Co^{2+} in solution. These observations are indicative of the *in situ* formation of an oxygen evolving catalyst. The electrocatalysis was performed at 1.29 V vs. NHE in a phosphate buffer solution using the catalyst film-coating ITO electrode in a gas tight electrochemical cell. The O_2 concentration in the headspace was measured by a fluorescent sensor. The amount of O_2 evolved increased linearly with time and was quantitatively consistent with the amount of charge passed during the electrocatalysis, showing 100% Faraday efficiency. Scanning electron microscope (SEM) observation showed that the electrodeposited film consist of particles that have coalesced into a thin film with individual micrometer-size particles on top of the film. The film thickness at the maximum activity under the electrolysis conditions was 2 μm. X-ray diffraction (XRD) pattern of the film showed broad amorphous features. The microanalytical elemental analysis data of the electrodeposited material indicates 2.1:1.0:0.8 of Co:P:K in a mole ratio. An X-ray absorption spectroscopy (XAS) technique was employed to reveal the oxidation state of Co, the coordination environments and the dominating structural motif of the Co catalyst film [22]. XAS data suggest that its central structural unit is a cluster of interconnected complete or incomplete Co^{III}-oxo cubanes (Fig. 7). Potassium ligation to Co-bridging oxygen atoms could result in $Co_3K(\mu\text{-}O)_4$ cubanes, in analogy to the $Mn_3Ca(\mu\text{-}O)_4$ cubane motif proposed for the photosynthetic OEC composed of a manganese-oxo cluster.

3. Conclusions and future scope

The current research on water oxidation chemistry has been based on two main interests: (1) seeking a practical catalyst for water oxidation for an artificial photosynthetic device, (2) providing a key model reaction to understand the O_2 production mechanism in photosynthesis. In the recent decade, great progress on water oxidation chemistry has been made, in the context of the recent energy and environmental problems and advances in the X-ray crystallographic analysis of photosynthetic OEC. Today, the research interests on water oxidation chemistry are expanding to electrocatalysis and photocatalysis, as the related impressive examples introduced in this review. The important features of the catalytic aspects of electrochemical and photochemical water oxidation are briefly summarized in Table 1 to compare them more easily. The catalytic aspects described here provide new concepts and present essential problems that are essential to resolve to design an artificial photosynthetic device. However, we are still a long way from establishing a photocatalyst system for water oxidation available for a practical device of artificial photosynthesis. The importance of developing an active and robust catalyst for water oxidation increases more than ever before, and critical advances on electron transfer between a water oxidation catalyst and a photoexcitation center are expected. Development of a new photoexcitation system in addition to a decent catalyst for water oxidation is key task for an artificial photosynthetic device.

Acknowledgments

Funding from Grant-in-Aid for Scientific Research (C) from The Ministry of Education, Culture, Sports, Science and Technology (No. 20550058) is gratefully acknowledged.

References

[1] N.S. Lewis, D.G. Nocera, Proc. Natl. Acad. Sci. U.S.A. 103 (2006) 15729.
[2] T.J. Meyer, Acc. Chem. Res. 22 (1989) 163.
[3] J.H. Alstrum-Acevedo, M.K. Brennaman, T.J. Meyer, Inorg. Chem. 44 (2005) 6802.
[4] M. Yagi, M. Kaneko, Chem. Rev. 101 (2001) 21.
[5] R. Manchanda, G.W. Brudvig, R.H. Crabtree, Coord. Chem. Rev. 144 (1995) 1.
[6] W. Ruettinger, G.C. Dismukes, Chem. Rev. 97 (1997) 1.
[7] S. Mukhopadhyay, S.K. Mandal, S. Bhaduri, W.H. Armstrong, Chem. Rev. 104 (2004) 3981.
[8] C.W. Cady, R.H. Crabtree, G.W. Brudvig, Coord. Chem. Rev. 252 (2008) 444.
[9] M. Yagi, A. Syouji, S. Yamada, M. Komi, H. Yamazaki, S. Tajima, Photochem. Photobiol. Sci. 8 (2009) 139.
[10] R. Brimblecombe, G.C. Dismukes, G.F. Swiegers, L. Spiccia, Dalton Trans. (2009) 9374.
[11] V.K. Yachandra, K. Sauer, M.P. Klein, Chem. Rev. 96 (1996) 2927.
[12] J.P. McEvoy, G.W. Brudvig, Chem. Rev. 106 (2006) 4455.
[13] J. Dasgupta, G.M. Ananyev, G.C. Dismukes, Coord. Chem. Rev. 252 (2008) 347.
[14] N. Kamiya, J.-R. Shen, Proc. Natl. Acad. Sci. U.S.A. 100 (2003) 98.
[15] K.N. Ferreira, T.M. Iverson, K. Maghlaoui, J. Barber, S. Iwata, Science 303 (2004) 1831.
[16] B. Loll, J. Kern, W. Saenger, A. Zouni, J. Biesiadka, Nature 438 (2005) 1040.
[17] J. Yano, J. Kern, K. Sauer, M.J. Latimer, Y. Pushkar, J. Biesiadka, B. Loll, W. Saenger, J. Messinger, A. Zouni, V.K. Yachandra, Science 314 (2006) 821.
[18] M.W. Kanan, Y. Surendranath, D.G. Nocera, Chem. Soc. Rev. 38 (2009) 109.
[19] M.W. Kanan, D.G. Nocera, Science 321 (2008) 1072.
[20] Y. Surendranath, M. Dinca, D.G. Nocera, J. Am. Chem. Soc. 131 (2009) 2615.
[21] D.A. Lutterman, Y. Surendranath, D.G. Nocera, J. Am. Chem. Soc. 131 (2009) 3838.
[22] M. Risch, V. Khare, I. Zaharieva, L. Gerencser, P. Chernev, H. Dau, J. Am. Chem. Soc. 131 (2009) 6936.
[23] J. Limburg, J.S. Vrettos, L.M. Liable-Sands, A.L. Rheingold, R.H. Crabtree, G.W. Brudvig, Science 283 (1999) 1524.
[24] J. Limburg, J.S. Vrettos, H.Y. Chen, J.C. de Paula, R.H. Crabtree, G.W. Brudvig, J. Am. Chem. Soc. 123 (2001) 423.
[25] R. Tagore, H. Chen, H. Zhang, R.H. Crabtree, G.W. Brudvig, Inorg. Chim. Acta 360 (2007) 2983.
[26] M. Yagi, K. Narita, J. Am. Chem. Soc. 126 (2004) 8084.
[27] P. Kurz, G. Berggren, M.F. Anderlund, S. Styring, Dalton Trans. (2007) 4258.
[28] C. Baffert, S. Romain, A. Richardot, J.-C. Lepretre, B. Lefebvre, A. Deronzier, M.-N. Collomb, J. Am. Chem. Soc. 127 (2005) 13694.
[29] K. Narita, T. Kuwabara, K. Sone, K. Shimizu, M. Yagi, J. Phys. Chem. B 110 (2006) 23107.
[30] M. Yagi, K. Narita, S. Maruyama, K. Sone, T. Kuwabara, K.-i. Shimizu, Biochim. Biophys. Acta Bioenerg. 1767 (2007) 660.
[31] M. Yagi, Abstract Book CD-ROM, in: 88th Spring Meeting of Chemical Society of Japan (CSJ), 5, 2008, p. S4.
[32] W.F. Ruettinger, C. Campana, G.C. Dismukes, J. Am. Chem. Soc. 119 (1997) 6670.
[33] W. Ruettinger, G.C. Dismukes, Inorg. Chem. 39 (2000) 1021.

[34] W. Ruettinger, M. Yagi, K. Wolf, S. Bernasek, G.C. Dismukes, J. Am. Chem. Soc. 122 (2000) 10353.
[35] M. Yagi, K.V. Wolf, P.J. Baesjou, S.L. Bernasek, G.C. Dismukes, Angew. Chem. Int. Ed. 40 (2001) 2925.
[36] R. Brimblecombe, G.F. Swiegers, G.C. Dismukes, L. Spiccia, Angew. Chem. Int. Ed. 47 (2008) 7335.
[37] R. Brimblecombe, D.R.J. Kolling, A.M. Bond, G.C. Dismukes, G.F. Swiegers, L. Spiccia, Inorg. Chem. 48 (2009) 7269.
[38] R. Brimblecombe, A.M. Bond, G.C. Dismukes, G.F. Swiegers, L. Spiccia, Phys. Chem. Chem. Phys. 11 (2009) 6441.
[39] G.E. Swiegers, J.H. Huang, R. Brimblecombe, J. Chen, G.C. Dismukes, U.T. Mueller-Westerhoff, L. Spiccia, G.G. Wallace, Chem. Eur. J. 15 (2009) 4746.
[40] G.C. Dismukes, R. Brimblecombe, G.A.N. Felton, R.S. Pryadun, J.E. Sheats, L. Spiccia, G.F. Swiegers, Acc. Chem. Res. 42 (2009) 1935.
[41] J.-Z. Wu, F. De Angelis, T.G. Carrell, G.P.A. Yap, J. Sheats, R. Car, G.C. Dismukes, Inorg. Chem. 45 (2006) 189.
[42] M. Yagi, S. Tokita, K. Nagoshi, I. Ogino, M. Kaneko, J. Chem. Soc. Faraday Trans. 92 (1996) 2457.
[43] M. Yagi, K. Kinoshita, M. Kaneko, J. Phys. Chem. 100 (1996) 11098.
[44] M. Yagi, K. Kinoshita, M. Kaneko, J. Phys. Chem. B 101 (1997) 3957.
[45] M. Yagi, K. Nagoshi, M. Kaneko, J. Phys. Chem. B 101 (1997) 5143.
[46] M. Yagi, N. Sukegawa, M. Kasamastu, M. Kaneko, J. Phys. Chem. B 103 (1999) 2151.
[47] M. Yagi, N. Sukegawa, M. Kaneko, J. Phys. Chem. B 104 (2000) 4111.
[48] M. Yagi, Y. Osawa, N. Sukegawa, M. Kaneko, Langmuir 15 (1999) 7406.
[49] S.W. Gersten, G.J. Samuels, T.J. Meyer, J. Am. Chem. Soc. 104 (1982) 4029.
[50] F. Liu, J.J. Concepcion, J.W. Jurss, T. Cardolaccia, J.L. Templeton, T.J. Meyer, Inorg. Chem. 47 (2008) 1727.
[51] J.K. Hurst, J.L. Cape, A.E. Clark, S. Das, C. Qin, Inorg. Chem. 47 (2008) 1753.
[52] F.P. Rotzinger, S. Munavalli, P. Comte, J.K. Hurst, M. Graetzel, F.-J. Pern, A.J. Frank, J. Am. Chem. Soc. 109 (1987) 6619.
[53] P. Comte, M.K. Nazeeruddin, F.P. Rotzinger, A.J. Frank, M. Graetzel, J. Mol. Catal. 52 (1989) 63.
[54] K. Nagoshi, S. Yamashita, M. Yagi, M. Kaneko, J. Mol. Catal. A: Chem. 144 (1999) 71.
[55] J.P. Collin, J.P. Sauvage, Inorg. Chem. 25 (1986) 135.
[56] T.J. Meyer, M.H.V. Huynh, Inorg. Chem. 42 (2003) 8140.
[57] D. Geselowitz, T.J. Meyer, Inorg. Chem. 29 (1990) 3894.
[58] J.A. Gilbert, D.S. Eggleston, W.R. Murphy, D.A. Geselowitz, S.W. Gersten, D.J. Hodgson, T.J. Meyer, J. Am. Chem. Soc. 107 (1985) 3855.
[59] C.W. Chronister, R.A. Binstead, J.F. Ni, T.J. Meyer, Inorg. Chem. 36 (1997) 3814.
[60] R.A. Binstead, C.W. Chronister, J.F. Ni, C.M. Hartshorn, T.J. Meyer, J. Am. Chem. Soc. 122 (2000) 8464.
[61] H. Yamada, J.K. Hurst, J. Am. Chem. Soc. 122 (2000) 5303.
[62] Y. Lei, J.K. Hurst, Inorg. Chim. Acta 226 (1994) 179.
[63] H. Yamada, W.F. Siems, T. Koike, J.K. Hurst, J. Am. Chem. Soc. 126 (2004) 9786.
[64] F. Liu, T. Cardolaccia, B.J. Hornstein, J.R. Schoonover, T.J. Meyer, J. Am. Chem. Soc. 129 (2007) 2446.
[65] C. Sens, I. Romero, M. Rodriguez, A. Llobet, T. Parella, J. Benet-Buchholz, J. Am. Chem. Soc. 126 (2004) 7798.
[66] R. Zong, R.P. Thummel, J. Am. Chem. Soc. 127 (2005) 12802.
[67] T. Wada, K. Tsuge, K. Tanaka, Angew. Chem. Int. Ed. 39 (2000) 1479.
[68] T. Wada, K. Tsuge, K. Tanaka, Inorg. Chem. 40 (2001) 329.
[69] Reprinted with permission from ref Copyright c 2000 WILEY-VCH Verlag GmbH & Co. KGaA.
[70] A. Sartorel, M. Carraro, G. Scorrano, R. De Zorzi, S. Geremia, N.D. McDaniel, S. Bernhard, M. Bonchio, J. Am. Chem. Soc. 130 (2008) 5006.
[71] Y.V. Geletii, B. Botar, P. Koegerler, D.A. Hillesheim, D.G. Musaev, C.L. Hill, Angew. Chem. Int. Ed. 47 (2008) 3896.
[72] Y.V. Geletii, Z. Huang, Y. Hou, D.G. Musaev, T. Lian, C.L. Hill, J. Am. Chem. Soc. 131 (2009) 7522.
[73] S.W. Kohl, L. Weiner, L. Schwartsburd, L. Konstantinovski, L.J.W. Shimon, Y. Ben-David, M.A. Iron, D. Milstein, Science 324 (2009) 74.
[74] A. Harriman, I.J. Pickering, J.M. Thomas, P.A. Christensen, J. Chem. Soc. Faraday Trans. 1 84 (1988) 2795.
[75] J. Kiwi, M. Graetzel, Angew. Chem. Int. Ed. Engl. 17 (1978) 860.
[76] J. Kiwi, M. Graetzel, Angew. Chem. Int. Ed. Engl. 18 (1979) 624.
[77] A. Mills, N. McMurray, J. Chem. Soc. Faraday Trans. 1 84 (1988) 379.
[78] G. Beni, L.M. Schiavone, J.L. Shay, W.C. Dautremont-Smith, B.S. Schneider, Nature 282 (1979) 281.
[79] F. Hine, M. Yasuda, T. Noda, T. Yoshida, J. Okuda, J. Electrochem. Soc. 126 (1979) 1439.
[80] A. Harriman, J.M. Thomas, New J. Chem. 11 (1987) 757.
[81] M. Hara, C.C. Waraksa, J.T. Lean, B.A. Lewis, T.E. Mallouk, J. Phys. Chem. A 104 (2000) 5275.
[82] N.D. Morris, M. Suzuki, T.E. Mallouk, J. Phys. Chem. A 108 (2004) 9115.
[83] N.D. Morris, T.E. Mallouk, J. Am. Chem. Soc. 124 (2002) 11114.
[84] M. Yagi, E. Tomita, S. Sakita, T. Kuwabara, K. Nagai, J. Phys. Chem. B 109 (2005) 21489.
[85] T. Kuwabara, E. Tomita, S. Sakita, D. Hasegawa, K. Sone, M. Yagi, J. Phys. Chem. C 112 (2008) 3774.
[86] I. Ogino, K. Nagoshi, M. Yagi, M. Kaneko, J. Chem. Soc. Faraday Trans. 92 (1996) 3431.
[87] M. Yagi, E. Tomita, T. Kuwabara, J. Electroanal. Chem. 579 (2005) 83.
[88] T. Nakagawa, N.S. Bjorge, R.W. Murray, J. Am. Chem. Soc. 131 (2009) 15578.
[89] T. Nakagawa, C.A. Beasley, R.W. Murray, J. Phys. Chem. C 113 (2009) 12958.
[90] M. Graetzel, K. Kalyanasundaram, Curr. Sci. 66 (1994) 706.
[91] M. Graetzel, Inorg. Chem. 44 (2005) 6841.
[92] W.J. Younpblood, S.H.A. Lee, Y. Kobayashi, E.A. Hernandez-Pagan, P.G. Hoertz, T.A. Moore, A.L. Moore, D. Gust, T.E. Mallouk, J. Am. Chem. Soc. 131 (2009) 926.